Macromolecules

pubs.acs.org/Macromolecules Article

One-Step Synthesis of a Degradable Thermoplastic Elastomer with Gradient Sequence via Chiral Brønsted Acid-Mediated Cationic Copolymerization of Vinyl Ether Monomer Mixtures

Yuqin Zhou, Yangyang Sun, Yanping Zhang,* and Miao Hong*

Cite This: Macromolecules 2024, 57, 7227−7236 Read Online

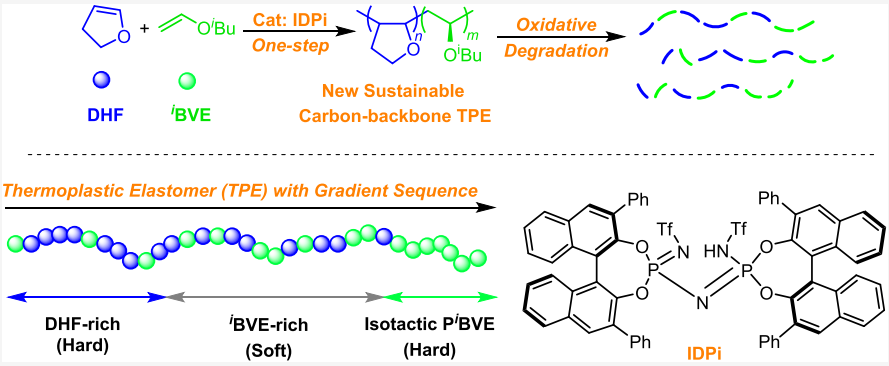

ABSTRACT: This contribution presents the facile synthesis of a new carbon-backbone thermoplastic elastomer (TPE) with on-demand degradability via one-step cationic copolymerization from biorenewable isobutyl vinyl ether (^{i}BVE) and 2,3-dihydrofuran (DHF) monomer mixtures. The utilization of imidodiphosphorimidate (IDPi), a strong organic Brønsted acid featuring a highly sterically demanding chiral pocket, as a single-component organic catalyst is the key to this achievement, which can bias the polymerization reactivity of comonomers, allow the copolymerization to proceed in a relatively controlled way, and render isotactic enchainment for the ^{i}BVE comonomer. Accordingly, DHF exhibits a much faster polymerization rate than ^{i}BVE during the copolymerization as opposed to their homopolymerizations (^{i}BVE ≫ DHF), and a series of DHF/^{i}BVE gradient copolymers with a hard (DHF-rich)−soft (^{i}BVE-rich)−hard (neat-isotactic P^{i}BVE) structure have been conveniently synthesized using a one-step approach. Structure−property evaluations reveal that the gradient copolymer, obtained by the copolymerization with a $[DHF]_0/[^iBVE]_0$ feed ratio of 2000:6000, possesses good thermal (T_d = 309 °C, T_m ≈ 70 °C, T_g ≈ −16 to 30 °C) and elastomeric properties (σ_B = 5.73 MPa, ε_B = 880%) and yet is capable of degrading in the presence of Fenton reagent, thus successfully constructs a new carbon-backbone TPE with high performance and on-demand degradability for the first time from poly(vinyl ether)-based gradient copolymers.

■ INTRODUCTION

Thermoplastic elastomers (TPEs) are essential polymeric materials which generally display high elastomeric properties like vulcanized rubbers in use but possess (re)processability like plastics at high temperature.[1−4] With a predicted annual production of 5.55 million tons in 2026,[5] TPEs can find wide applications in electronic components, sporting goods, medical devices, food containers, seals, etc. However, TPE materials are facing two key challenges at present. First, thermoplastic olefins (TPOs), acrylonitrile-butadiene rubbers (NBRs), and styrenic block copolymers (SBCs) account for over 70% of TPEs in the consumer market,[6] but their inherently inert C−C-bonded backbones make them resistant to degradation which ultimately leads to the accumulation and persistence of postconsumer wastes. To impart degradability to TPEs, recent advances and studies have centered on the development of TPEs with labile group-containing main chains (e.g., polyester-based TPEs).[7−13] Nevertheless, the labile groups in the main chains generally bring about detrimental effects on the physical properties and durability of the resultant polymers. Therefore, the development of TPEs, which maintain all-carbon backbones for practical use yet possess on-demand degradability under certain stimuli after end of life, provides an important alternative but remains a rare instance. Second, the traditional synthesis of TPEs usually relies on the sequential addition of

Received: April 16, 2024
Revised: June 27, 2024
Accepted: July 11, 2024
Published: July 24, 2024

Scheme 1. One-Step Synthesis of Carbon-Backbone TPEs with Gradient Sequence via Chiral IDPi-Mediated Cationic Polymerization of DHF and ^{i}BVE Monomer Mixtures in This Work

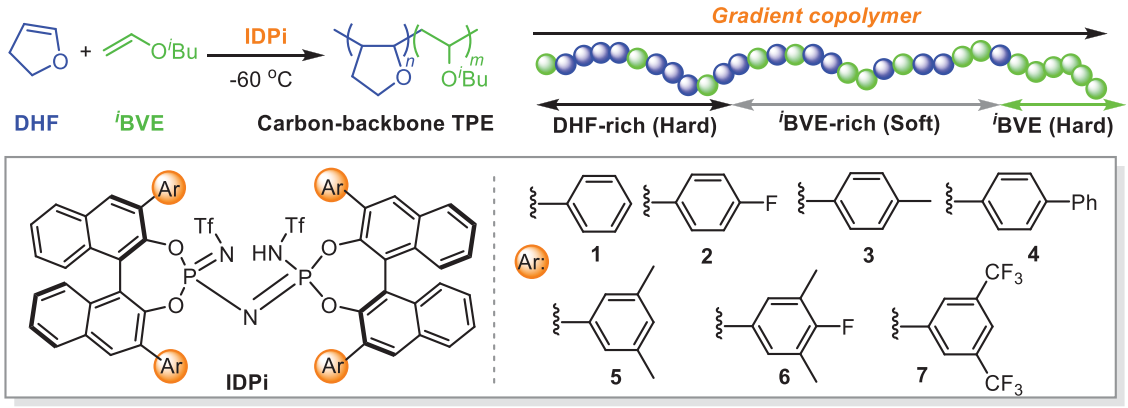

Table 1. Representative Homopolymerization Results for IDPis[a]

run	IDPi	monomer	time (h)	temp. (°C)	conv.[b] (%)	M_n[c] (kg/mol)	$Đ$[c]
1	**1**	DHF	24	−78	87	41.0	1.49
2	**1**	^{i}BVE	0.167	−78	>99	153.5	1.09
3	**1**	DHF	0.5	−60	56	21.0	1.53
4	**1**	DHF	8	−60	>99	33.3	1.59
5	**2**	DHF	8	−60	>99	17.5	1.44
6	**3**	DHF	8	−60	>99	23.8	1.53
7	**4**	DHF	8	−60	94	12.4	1.88
8	**5**	DHF	8	−60	97	21.8	1.51
9	**6**	DHF	8	−60	38	18.8	1.36
10	**7**	DHF	8	−60	0		

[a]Polymerization conditions: IDPi = 2 μmol, $[\text{monomer}]_0/[\text{IDPi}]_0$ = 1000:1, toluene as the solvent, V_{total} = 2 mL. [b]Monomer conversions were determined by ^{1}H NMR. [c]Number-average molecular weight (M_n) and molecular-weight distribution ($Đ = M_w/M_n$) were determined by GPC relative to PMMA standards in THF at 40 °C.

comonomers to achieve block copolymers with microphase-segregated structures. In sharp contrast, the direct and one-step polymerization from one-pot comonomer mixtures to synthesize TPEs exhibits practical and technological benefits[14−23] but remains a significant challenge.

Vinyl ethers and their cyclic analogues (e.g., 2,3-dihydrofuran, DHF) can be synthesized from biorenewable alcohols and have been recognized as emerging bioderived monomers for sustainable polymers.[24−26] More importantly, recent reports have demonstrated that the incorporation of vinyl ethers can impart degradability to carbon-backbone polymers. For example, Ouchi and co-workers achieved the degradation of acrylate polymers by the utilization of vinyl ether comonomers as the trigger whose pendant C−H bonds are active for hydrogen atom transfer to generate backbone radicals for degradation.[27] Moreover, Fors et al. demonstrated poly(2,3-dihydrofuran), produced from cationic polymerization of DHF, as a strong thermoplastic that can undergo oxidative degradation in the presence of Fenton reagent.[26] Both notable examples give a hint that vinyl ether and DHF are promising monomers for constructing carbon-backbone TPEs with on-demand degradability.

In this contribution, we aim at the one-step synthesis of degradable TPEs with all-carbon backbones from vinyl ether and DHF monomer mixtures (Scheme 1). To realize this goal, we herein reason that the utilization of imidodiphosphorimidate (IDPi, Scheme 1),[28,29] a strong organic Brønsted acid ($pK_a \leq 4.5$ in MeCN) featuring a highly sterically demanding chiral pocket, as the catalyst holds great potential, thanks to its following benefits or advantages. First, an enzyme-like "electrostatic lock-and-key" binding mode of counterions derived from IDPi, which has shown capability for mediating highly enantioselective transformations in the Hosomi−Sakurai reaction,[30] [4 + 2]-cycloaddition,[31] and the Mukaiyama−Michael reaction,[32] might bias the reactivity of comonomers during one-step cationic polymerization to produce TPEs with block or gradient sequence from vinyl ether and DHF monomer mixtures. Second, IDPi has also been demonstrated as a robust single-component organic catalyst for the highly isotactic cationic polymerization of various alkyl vinyl ethers. Compared to the corresponding amorphous analogues, the resultant isotactic polar polymers show enhanced performance with regard to their thermal and mechanical properties comparable to that of commercial low-density polyethylene.[33,34] Therefore, the utilization of IDPi as the catalyst would produce an isotactic vinyl ether segment or block which should impart superior properties to high-performance TPEs.

Herein, the investigation into the effect of IDPi structures on copolymerization behaviors has led to the disclosure of IDPi-**1** (Scheme 1) which can bias the polymerization reactivity of isobutyl vinyl ether (^{i}BVE) and DHF comonomers, allow the copolymerization to proceed in a relatively controlled way, and render isotactic enchainment for the ^{i}BVE comonomer. Accordingly, a series of DHF/^{i}BVE gradient copolymers with a hard (DHF-rich)−soft (^{i}BVE-rich)−hard (neat-isotactic P^{i}BVE) structure have been conveniently synthesized in a one-step approach. The structure−property relationship of

https://doi.org/10.1021/acs.macromol.4c00857
Macromolecules 2024, 57, 7227−7236

Table 2. Representative Copolymerization Results for IDPi-1[a]

run	$[DHF]_0/[^iBVE]_0/[IDPi\text{-}1]_0$	time (min)	conv.%[b] (DHF)	conv.%[b] (^{i}BVE)	$M_{n,theo}$[c] (kg/mol)	M_n[d] (kg/mol)	Đ[d]
1[e]	250:750:1	1440	97	41	47.8	44.2	1.33
2	250:750:1	150	>99	98	90.8	92.8	1.88
3	250:750:1	20	59	15	21.3	21.8	1.82
4	250:750:1	40	78	34	39.0	30.0	1.67
5	250:750:1	60	85	39	44.5	35.7	1.78
6	250:750:1	90	94	54	57.1	46.5	1.70
7	250:750:1	100	96	66	66.8	54.1	1.82
8	250:750:1	110	98	71	70.5	64.3	1.72
9	250:750:1	120	>99	80	77.6	67.9	1.75
10	500:500:1	10	46	12	22.1	25.8	1.38
11	500:500:1	30	62	20	31.7	29.6	1.40
12	500:500:1	60	83	41	49.6	38.9	1.45
13	500:500:1	90	96	63	65.2	53.4	1.46
14	500:500:1	180	>99	>99	84.3	61.8	1.52

[a]Polymerization conditions: IDPi-**1** = 2 μmol, V_{total} = 2 mL, toluene as the solvent, Temp. = −60 °C. [b]Monomer conversions were determined by ^{1}H NMR. [c]$M_{n,theo}$ = MW(DHF) × $[DHF]_0/[IDPi\text{-}1]_0$ × conv.(DHF)% × + MW(^{i}BVE) × $[^iBVE]_0/[IDPi\text{-}1]_0$ × conv.(^{i}BVE)% + MW(−OMe). [d]Number-average molecular weight (M_n) and molecular-weight distribution (Đ = M_w/M_n) were determined by GPC relative to PMMA standards in THF at 40 °C. [e]Temp. = −78 °C.

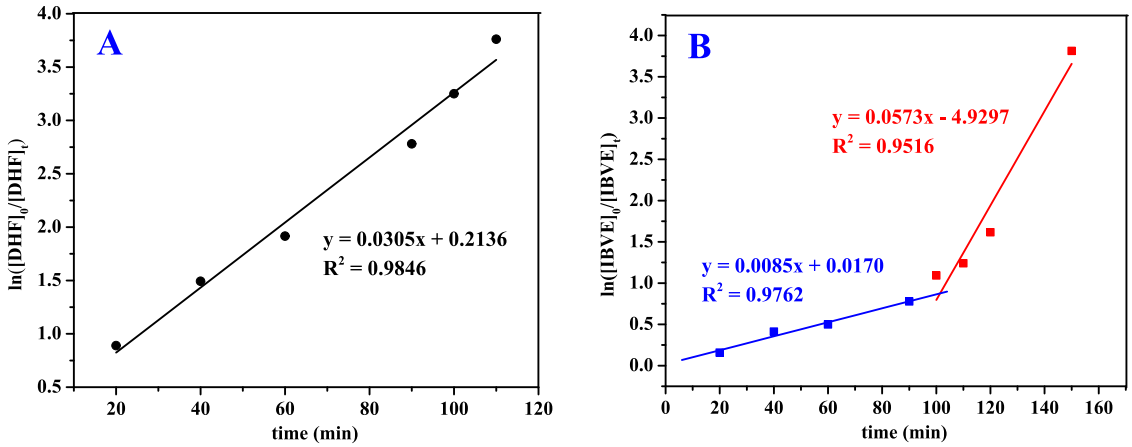

Figure 1. Kinetic analysis of DHF (A) and ^{i}BVE (B) during the copolymerization with a $[DHF]_0/[^iBVE]_0$ feed ratio of 250:750 using IDPi-**1** as the catalyst.

these gradient copolymers has also been evaluated, affording a new sustainable carbon-backbone TPE that is robust in use but also on-demand degradable under certain stimuli after use.

■ RESULTS AND DISCUSSION

Cationic Copolymerization of DHF with ^{i}BVE by IDPis. According to literature procedures,[35,36] we synthesized a series of chiral IDPis with different electronic nature and steric hindrance (Scheme 1) through a facile one-pot reaction of 3,3′-substituted binaphthol derivatives with $P(NTf)Cl_3$ and homopolymerization of acyclic vinyl ethers by IDPis,[33,34] while their polymerization behaviors of cyclic analogues, as represented by DHF, remain unknown yet. Therefore, before the evaluation of one-pot sequence-controlled copolymerization, we first investigated IDPi-mediated homopolymerization of DHF, and the representative results are summarized in Table 1. With a $[DHF]_0/[IDPi]_0$ ratio of 1000:1, IDPi-**1** was capable of polymerizing DHF at −78 °C without the addition of a co-initiator or an activator (Table 1, run 1), indicating that IDPi-**1** can act as a single-component organic catalyst. However, compared to rapid and quantitative polymerization of ^{i}BVE (10 min, conv. >99%, Table 1, run 2), IDPi-**1** exhibited much lower activity toward DHF polymerization under similar conditions (24 h, conv. = 87%), presumably due to a slower initiation process (vide infra) because of the hindered addition reaction between the double bond of the bulkier DHF monomer and the proton of sterically confined IDPi. Notably, the polymerization significantly accelerated when the reaction temperature was increased from −78 to −60 °C, where a monomer conversion of 56% can be achieved in 0.5 h and quantitative conversion was accomplished in 8 h (Table 1, runs 3 and 4).

The screening of IDPi scope revealed that IDPi-**1** is unique in efficiently polymerizing DHFs into a relatively high-molecular-weight (MW) polymer. The introduction of a substituent in the *para*-position of the benzene ring (IDPi-**2**−**4**, Table 1, runs 5−7) decreased the MW of the resultant polymers, while the introduction of the substituents in the 3,5-position of the benzene ring (IDPi-**5**−**7**, Table 1, runs 8−10) led to low or no polymerization activity with reduced MWs. Especially, IDPi-**7** with two electron-withdrawing groups ($-CF_3$) in the 3,5-position was incapable of initiating DHF polymerization.

Having established IDPi-**1** as an efficient single-component organic catalyst for DHF homopolymerization, one-pot

https://doi.org/10.1021/acs.macromol.4c00857
Macromolecules 2024, 57, 7227−7236

sequence-controlled copolymerization of ^{i}BVE and DHF by IDPi-**1** was subsequently investigated. With a $[DHF]_0/[^iBVE]_0/[IDPi\text{-}1]_0$ ratio of 250:750:1, IDPi-**1** was able to convert 97% of DHF and 41% of ^{i}BVE into a copolymer within 24 h when the polymerization was carried out at −78 °C (Table 2, run 1). Similar to the homopolymerization of DHF, elevating the reaction temperature to −60 °C can notably enhance the polymerization activity, in which quantitative conversions of both DHF and ^{i}BVE were accomplished in 3 h (Table 2, run 2).

To obtain monomer sequence of the copolymers, the kinetic study of this copolymerization was performed (Table 2, runs 2−9). As depicted in Figure 1A, DHF conversion followed first-order kinetics during the copolymerization with an apparent rate constant (k_{obs}) of 0.0305 min^{-1}. Different from that of DHF, the conversion of ^{i}BVE proceeded via two reaction stages (Figure 1B). At the first stage, the k_{obs} of ^{i}BVE was determined to be 0.0085 min^{-1} in the presence of DHF. After complete consumption of DHF, the conversion of ^{i}BVE moved to the second stage, and its k_{obs} significantly enhanced to 0.0573 min^{-1}, providing the P^{i}BVE segment accordingly. It is noteworthy that the polymerization rate of DHF was much faster than that of ^{i}BVE during the first stage of copolymerization, as opposed to their homopolymerizations (^{i}BVE ≫ DHF, vide supra). Moreover, it is also worth noting that the polymerization rate of DHF in copolymerization was much faster than that of DHF in homopolymerization (k_{obs} = 0.0265 min^{-1}, Figure S1), while the polymerization rate of ^{i}BVE at both stages of copolymerization was much slower than that of ^{i}BVE in homopolymerization (k_{obs} > 0.0154 s^{-1}, Figure S2).

The observation of substantially different polymerization rates of both DHF and ^{i}BVE between homopolymerization and copolymerization in this work is very intriguing. We speculated that, in homopolymerization, slower polymerization of DHF relative to that of ^{i}BVE is presumably due to a slower initiation process because of the hindered addition reaction between the double bond of the bulkier DHF monomer and the proton of sterically confined IDPi-**1**, though the propagation process of DHF should be faster than that of ^{i}BVE on account of its unique cyclic enol ether structure that makes DHF more nucleophilic to carbocation active species than linear ^{i}BVE. In the case of copolymerization, the presence of ^{i}BVE can facilitate initiation through the rapid addition reaction between IDPi-**1** and ^{i}BVE, immediately producing carbocation active species and IDPi-**1** counterions for subsequent propagation. Therefore, with the assistance of ^{i}BVE in facilitating initiation, the polymerization rate of DHF in copolymerization is accordingly higher than that of DHF in homopolymerization. The identical facilitating initiation by ^{i}BVE can also be observed in IDPi-**1**-mediated copolymerization of ^{i}BVE and 3,4-dihydro-2*H*-pyran (DHP), a sterically more hindered cyclic enol ether. In sharp contrast to the inactive homopolymerization of DHP by IDPi-**1** ($[DHP]_0/[IDPi\text{-}1]_0$ = 1000:1, 24 h), DHP was able to be polymerized in IDPi-**1**-mediated copolymerization of DHP and ^{i}BVE, despite its relatively lower conversion of 30% in 16 h, affording a copolymer with a M_n of 35.3 kg/mol and a $Đ$ of 1.50 ($[DHP]_0/[^iBVE]_0/[IDPi\text{-}1]_0$ = 250:750:1, conv.(^{i}BVE) = 94%). In consideration of the inactive homopolymerization of DHP, the propagation of DHP in copolymerization is thereby speculated to be enabled by facilitating initiation of ^{i}BVE. Moreover, stronger nucleophilicity of DHF relative to that of ^{i}BVE results in the deceleration of ^{i}BVE polymerization. Correspondingly, DHF tends to be preferentially polymerized over ^{i}BVE, and the polymerization rate of ^{i}BVE in copolymerization is much slower than its homopolymerization.

When changing the $[DHF]_0/[^iBVE]_0$ feed ratio from 250:750 to 500:500, it was found that IDPi-**1** also preferentially polymerized DHF over ^{i}BVE (Table 2, runs 10−14). For example, DHF conversion quickly reached 46% within 10 min, but in the meantime only 12% of ^{i}BVE was converted. After 90 min, near-quantitative conversion of DHF was achieved (96%), whereas 37% of ^{i}BVE still remained unpolymerized which required another 90 min to completely consume to afford a neat P^{i}BVE segment. Identical to 250:750, the copolymerization with a $[DHF]_0/[^iBVE]_0$ feed ratio of 500:500 also showed a first-order reaction of DHF with a k_{obs} of 0.0429 min^{-1} and two reaction stages of ^{i}BVE with k_{obs} values of 0.0110 and 0.0418 min^{-1} (Figure S3), also revealing a faster polymerization rate of DHF than ^{i}BVE and significant acceleration of ^{i}BVE polymerization after complete consumption of DHF.

Establishment of Gradient Sequence of the DHF/^{i}BVE Copolymer. On the basis of kinetic studies, copolymerizations are speculated to produce a copolymer with gradient sequence which consists of DHF-rich, ^{i}BVE-rich, and neat ^{i}BVE segments. To exclude the formation of homopolymer mixtures, diffusion-ordered spectroscopy (DOSY) was performed. As shown in Figure 2, the resultant product obtained by IDPi-**1**-mediated copolymerization only shows one diffusion coefficient, in sharp contrast to homopolymer mixtures of PDHF and P^{i}BVE which exhibit two diffusion coefficients, clearly demonstrating that a copolymer rather than homopolymer mixtures was formed. In addition, GPC curves of all copolymer samples produced during the copolymerizations under different comonomer feed ratios ($[DHF]_0/[^iBVE]_0$ = 250:750, 500:500) show relatively narrow and unimodal distributions, which gradually shift to the higher MW region with increasing monomer conversion (Figure 3), further confirming the formation of true copolymers. Therefore, the kinetic studies in combination of DOSY and GPC analyses unequivocally demonstrate that DHF/^{i}BVE copolymers with a gradient sequence were produced.

Moreover, it is also important that IDPi-**1** has good control over MW, as evidenced by the observation of linear growth of copolymer M_n with increasing monomer conversion (Figure 3). The sterically demanding chiral counterion derived from IDPi-**1** is proposed to stabilize the carbocation propagation species via ion-pair interaction, thus effectively suppressing the chain transfer and termination side reactions.[37] Interestingly, there is two-stage linear growth for the copolymerization at a $[DHF]_0/[^iBVE]_0$ feed ratio of 250:750 (Figure 3, top), while the copolymerization at a $[DHF]_0/[^iBVE]_0$ feed ratio of 500:500 shows one linear region (Figure 3, bottom). Such difference should be caused by the MW difference between two monomers [100 (^{i}BVE) vs 70 (DHF) g/mol] as well as an excess of ^{i}BVE in feed in the former copolymerization, which led to a longer length of the neat P^{i}BVE segment after complete consumption of DHF. As a result, the switch from mainly DHF conversion to (near) neat ^{i}BVE conversion in the former copolymerization brings about the significant increase of MW, thus resulting in two linear regimes in the M_n vs conversion plot.

https://doi.org/10.1021/acs.macromol.4c00857
Macromolecules 2024, 57, 7227−7236

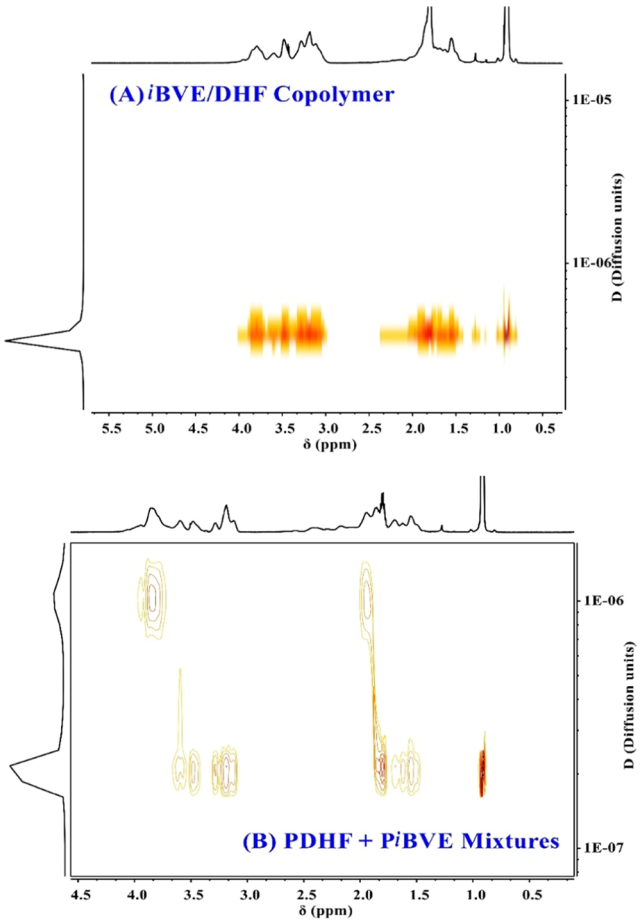

Figure 2. DOSY NMR spectra of the polymer product obtained by IDPi-**1**-mediated copolymerization with a $[DHF]_0/[^iBVE]_0$ feed ratio of 250:750 (A) and homopolymer mixtures of PDHF and P^{i}BVE (B).

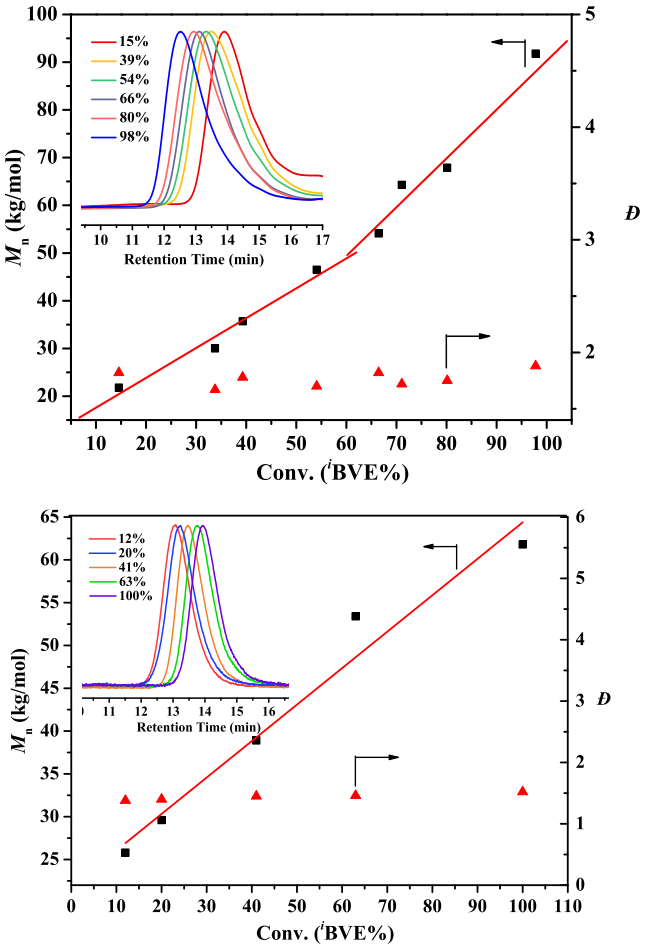

Figure 3. Plots of M_n and $Đ$ for the copolymer vs ^{i}BVE conversion (%) and insets are GPC curves for the copolymers produced at different ^{i}BVE conversions (Table 2): (top) $[DHF]_0/[^iBVE]_0$ = 250:750; (bottom) $[DHF]_0/[^iBVE]_0$ = 500:500.

To provide further evidence for the formation of gradient copolymers, the reactivity ratios of DHF and ^{i}BVE in IDPi-**1**-mediated copolymerizations were determined by the Meyer−Lowry method. Different from the conventional Fineman−Ross or Kelen−Tüdös method which is only valid at a low monomer conversion (approximately 5−10%), the Meyer−Lowry model can be calculated from kinetic polymerization data that span the full range of conversion.[38−42] Considering that a given copolymerization at low monomer conversion may not reach a steady-state concentration of the growing polymer and may not yet consume enough monomer to present a statistically meaningful and representative result, the Meyer−Lowry model is thus a more suitable method to determine the reactivity ratios of gradient copolymerizations. Accordingly, as shown in Tables S1−S2 and Figures S4−S5, the reactivity ratios of DHF and ^{i}BVE in the copolymerizations with different comonomer feed ratios were calculated to be 9.60 and 0.51 ($[DHF]_0/[^iBVE]_0$ = 250:750) as well as 6.32 and 0.62 ($[DHF]_0/[^iBVE]_0$ = 500:500). These values fit well with the gradient copolymerization behavior of $r_{DHF} > 1 > r_{iBVE}$.[38]

Structure−Property Relationship and Degradation Behavior of DHF/^{i}BVE Gradient Copolymers. To provide sufficient material for structure−property evaluations, copolymerizations with different $[DHF]_0/[^iBVE]_0$ feed ratios were scaled up, and multigram quantities of gradient copolymers with high MWs (167−547 kg/mol) were obtained (Table 3 and Figure S6). Microstructures of these copolymers as well as of PDHF and P^{i}BVE homopolymers were analyzed by ^{13}C NMR. As shown in Figures 4 and S7, IDPi-**1**-catalyzed homopolymerization of DHF at −60 °C yielded PDHF with *cis*- and *trans*-structures in a ratio of ca. 42:58. The glass-transition temperature of resultant PDHF (T_g = 140 °C), as examined by differential scanning calorimetry (DSC, Figure 5), is slightly higher than that produced by an organic acid of pentakis-(methoxycarbonyl)cyclopentadiene at room temperature reported by Fors et al. (T_g = 131 °C).[26] Moreover, ^{13}C NMR analysis reveals that P^{i}BVE produced by IDPi-**1** at −78 °C has relatively high isotacticity with an *m* value of 85% (Figures 4 and S8), identical to that of previous report (*m* = 88%).[34] Accordingly, despite the low degree of crystallinity, the resultant isotactic P^{i}BVE possesses a melting temperature (T_m) of 86 °C together with a low T_g value of −19 °C (Figure 5).

It is noteworthy that the copolymerization of ^{i}BVE with DHF by IDPi-**1** at −60 °C only slightly decreased the isospecificity of ^{i}BVE, affording P^{i}BVE segments with *m* values in the range of 78−83% (Figures 4 and S9−S13). DSC curves for the first-heating scans of these gradient copolymers display melting temperatures (T_ms) of ∼70 °C (Figure S14), which should correspond to isotactic P^{i}BVE segments that would behave as a hard block for thermoplastic elastomers (TPEs). Wide-angle X-ray diffraction (WAXD) patterns (Figures 5 and S15) reveal that the characteristic diffraction peaks of gradient

https://doi.org/10.1021/acs.macromol.4c00857
Macromolecules 2024, 57, 7227−7236

Table 3. Gradient Copolymer Samples with High MWs for Physical Property Measurements[a]

sample	$[DHF]_0/[^iBVE]_0/[IDPi\text{-}1]_0$	M_n[b] (kg/mol)	$Đ$[b]	m[c] (%)	σ_B[d] (MPa)	ε_B[d] (%)
$PDHF_{800}$-P^iBVE_{7200}	800:7200:1	547.3	1.67	78	1.71	1700
$PDHF_{1600}$-P^iBVE_{6400}	1600:6400:1	339.3	1.89	78	3.31	1200
$PDHF_{2000}$-P^iBVE_{6000}	2000:6000:1	296.4	2.05	81	5.73	880
$PDHF_{2400}$-P^iBVE_{5600}	2400:5600:1	291.7	2.15	81	6.36	590
$PDHF_{4000}$-P^iBVE_{4000}	4000:4000:1	167.3	1.98	83	37.1	5

[a]Polymerization conditions: IDPi-**1** = 2 μmol, V_{total} = 12 mL, toluene as the solvent, Temp. = −60 °C, conv.(DHF)% = conv.(^iBVE)% > 99% in 24 h. [b]Number-average molecular weight (M_n) and molecular-weight distribution ($Đ = M_w/M_n$) were determined by GPC relative to PMMA standards in THF at 40 °C. [c]Isotacticity (diad distribution) determined by quantitative ^{13}C NMR spectroscopy. [d]Tensile strength (σ_B) and elongation at break (ε_B) determined by the tensile test using a cross-head rate of 50 mm/min.

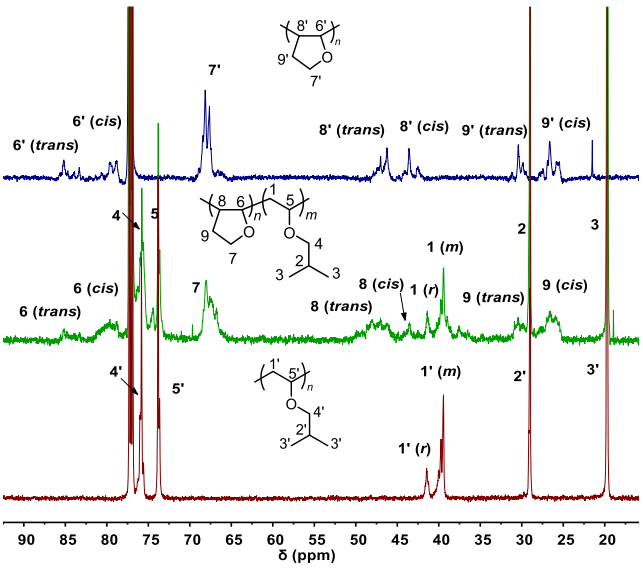

Figure 4. Overlap of quantitative ^{13}C NMR spectra of isotactic P^iBVE (bottom, Table 1, run 2), PDHF (top, Table 1, run 4), and gradient copolymer of $PDHF_{4000}$-P^iBVE_{4000} (middle, Table 3).

copolymers appear at 2θ values of 9.16, 10.80, 18.60, and 21.00°, similar to those of isotactic P^iBVE homopolymers (2θ: 9.06, 10.78, 18.42, and 21.02°) but in sharp contrast to broad diffraction signals at 12.80 and 19.30° in amorphous PDHF, further confirming the semicrystalline characteristic of P^iBVE segments in gradient copolymers. However, in the second-heating scan, gradient copolymers become amorphous by showing only T_gs. Interestingly, it is found that, except $PDHF_{4000}$-P^iBVE_{4000} that exhibits a single T_g of −10 °C, broad T_g ranges are observed for gradient copolymers by displaying onset temperatures of ca. −14 to −20 °C and terminal temperatures of 13−83 °C (Figure 5). The onset temperature presumably corresponds to the P^iBVE segment as it is close to the T_g value of the P^iBVE homopolymer, whereas the terminal temperature enhances with increasing DHF content which thus should be related to the DHF-rich segment that would also behave as a hard block for TPE. The observation of a broad T_g range in DHF/^iBVE copolymers, significantly different from those of random (single T_g) or block (generally independent T_gs and/or T_ms corresponding to homopolymer blocks) copolymers, provides further evidence for their gradient structures. Moreover, according to the above kinetic studies, the middle segments of these gradient copolymers are presumably attributed to ^iBVE-rich segments. Because of the disruption of the crystallization of P^iBVE by DHF, ^iBVE-rich segments are amorphous and exhibit T_g values below RT, which would act as soft blocks for TPE.

Having established the ^iBVE/DHF gradient copolymer possessing a hard (DHF-rich)−soft (^iBVE-rich)−hard (neat-P^iBVE) structure, their potential as the TPE was evaluated by tensile tests. As shown in Figure 6A and Table 3, it is found that the tensile properties of gradient copolymers highly depend on the polymer composition. For example, the $PDHF_{800}$-P^iBVE_{7200} copolymer serves as a TPE by displaying

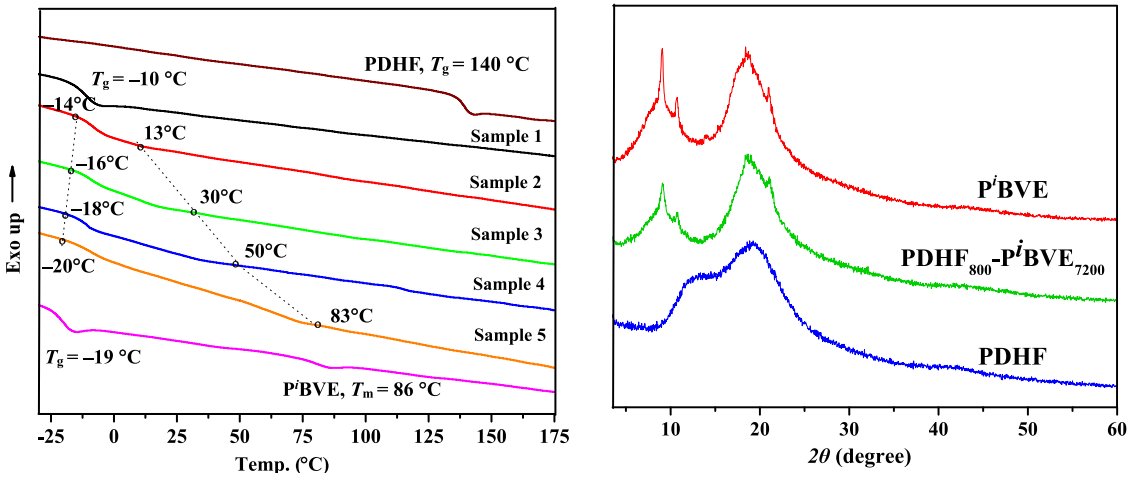

Figure 5. (Left) Overlay of second-heating-scan DSC curves of PDHF (Table 1, run 4), isotactic P^iBVE (Table 1, run 2), and gradient copolymers (samples 1−5 correspond to $PDHF_{800}$-P^iBVE_{7200}, $PDHF_{1600}$-P^iBVE_{6400}, $PDHF_{2000}$-P^iBVE_{6000}, $PDHF_{2400}$-P^iBVE_{5600}, and $PDHF_{4000}$-P^iBVE_{4000}, respectively); (right) overlay of WXRD profiles of isotactic P^iBVE, PDHF, and $PDHF_{800}$-P^iBVE_{7200} gradient copolymers.

https://doi.org/10.1021/acs.macromol.4c00857
Macromolecules 2024, 57, 7227−7236

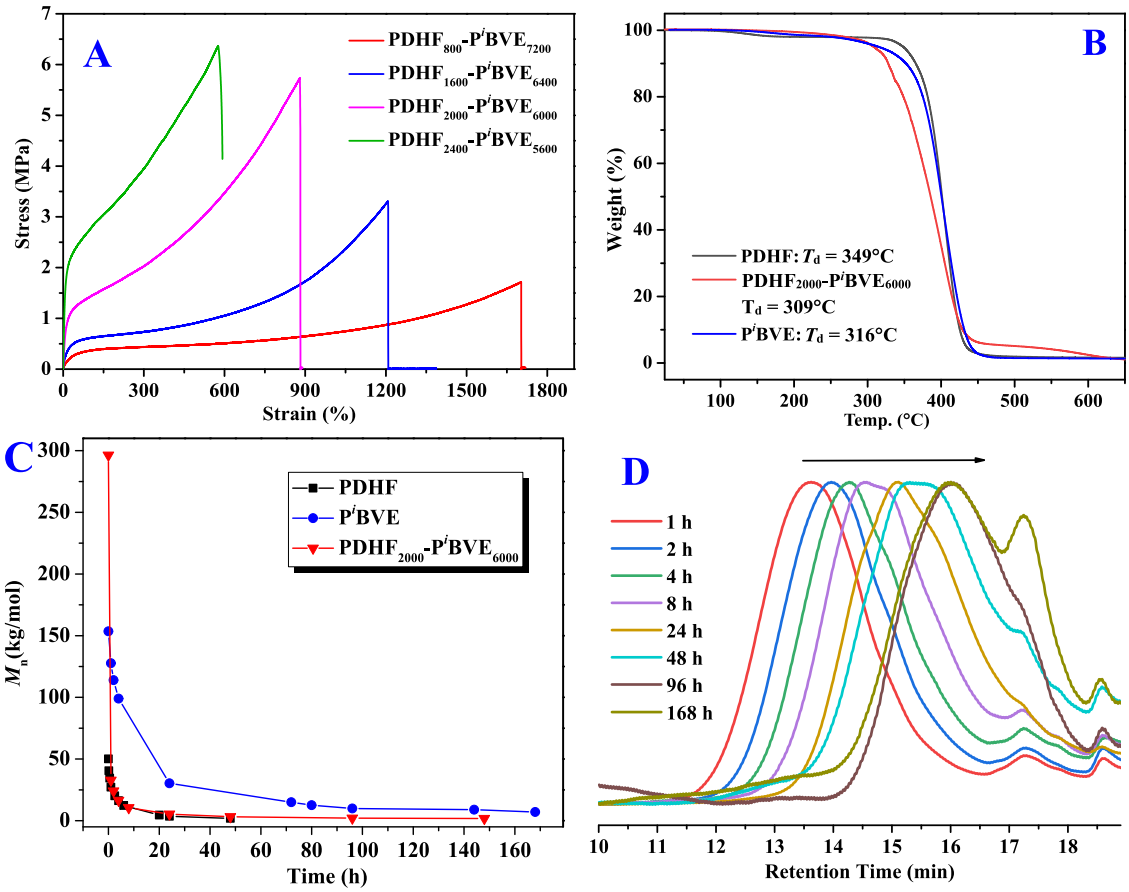

Figure 6. (A) Representative stress−strain curves of gradient copolymers; (B) TGA curves of PDHF, isotactic P^{i}BVE, and PDHF$_{2000}$-P^{i}BVE$_{6000}$; (C) monitoring the variation of M_ns of isotactic P^{i}BVE and PDHF$_{2000}$-P^{i}BVE$_{6000}$ during the degradation process. Plots of M_n of PDHF degradation product vs time are reported by Fors and co-workers,[26] which are provided for comparison; (D) GPC curves of degradation products of PDHF$_{2000}$-P^{i}BVE$_{6000}$ at different degradation times.

a very high elongation at break (ε_B) of 1700% without yield point, in sharp contrast to isotactic P^{i}BVE[43,44] and PDHF[26] homopolymers which behave as a strong and/or tough thermoplastic. However, this copolymer exhibits a low tensile strength (σ_B) of 1.71 MPa, presumably due to the short length of the DHF-rich hard block. With an increase of the DHF amount in the feed from a [DHF]$_0$/[^{i}BVE]$_0$ ratio of 800:7200 to 2400:5600, the resultant copolymers also behave as the TPEs with σ_B being gradually enhanced from 1.71 to 3.31, 5.73, and 6.36 MPa because of the increased length of the DHF-rich hard block, though ε_B decreased from 1700% to 1200%, 880%, and 590%, respectively. Interestingly, when the DHF amount was further increased in the feed with a [DHF]$_0$/[^{i}BVE]$_0$ ratio of 4000:4000, a shift from a TPE to a hard and brittle thermoplastic was observed. As shown in Figure S16, the resultant PDHF$_{4000}$-P^{i}BVE$_{4000}$ copolymer exhibits a high σ_B of 37.1 MPa but very low ε_B of only 5%, presumably on account of the short length of the ^{i}BVE-rich soft block. It is worth noting that a fine balance between σ_B (5.73 MPa) and ε_B (880%) has been achieved for the PDHF$_{2000}$-P^{i}BVE$_{6000}$ copolymer because of reasonable lengths of both soft and hard blocks. Remarkably, this gradient copolymer is a new high-performance TPE, the tensile property of which is superior to those of the PDHF-*b*-*atactic* P^{i}BVE-*b*-PDHF triblock copolymer analogue (σ_B = 4.30 MPa, ε_B = 570%)[25] and a poly(vinyl ether)-based block copolymer (σ_B = 4.85 MPa, ε_B = 475%)[45,46] reported previously and also in good competition with those of unfilled vulcanized acrylonitrile-butadiene rubber (NBR, σ_B: 3−7 MPa, ε_B: 350−800%).[47]

So far, reports on the utilization of gradient copolymers for TPEs are very rare[48−51] due to their generally inferior mechanical properties compared to their block copolymer analogues, which is presumably due to the relatively higher compatibility between different segments in gradient copolymers that results in more difficult microphase separation. In addition, to our knowledge, the synthesis of poly(vinyl ether)-based gradient copolymers via cationic copolymerizations for TPE application has not been reported yet. In this work, the utilization of IDPi-**1** not only realizes the one-step synthesis of TPEs via cationic copolymerization from monomer mixtures but also successfully constructs a high-performance TPE for the first time from poly(vinyl ether)-based gradient copolymers.

It is worth mentioning that the copolymerization of ^{i}BVE and DHF by a strong organic Brønsted acid HNTf$_2$ also produced the gradient copolymer [Table S3, 20 min: conv.(DHF) = 51%, conv.(^{i}BVE) = 23%; 90 min: conv.(DHF) = 94%, conv.(^{i}BVE) = 64%], despite its relatively lower gradient degree than IDPi-**1**-mediated copolymerization [Table 2: 20 min: conv.(DHF) = 59%, conv.(^{i}BVE) = 15%; 90 min: conv.(DHF) = 94%, conv.(^{i}BVE) = 54%]. Although both are gradient copolymers, the mechanical property of PDHF$_{2000}$-P^{i}BVE$_{6000}$ with a hard (DHF-rich)−soft (^{i}BVE-rich)−hard (*isotactic*-P^{i}BVE) structure obtained by IDPi-**1** is superior to

https://doi.org/10.1021/acs.macromol.4c00857
Macromolecules 2024, 57, 7227−7236

that of the gradient copolymer with a DHF-rich (hard)−^{i}BVE-rich (soft)−*atactic*-P^{i}BVE (soft) structure produced by $HNTf_2$ [σ_B = 2.83 MPa, ε_B = 824%, m (^{i}BVE) = 70%, M_n = 313.6 kg/mol, $Đ$ = 1.68, Figure S17]. This result clearly demonstrates that isotactic P^{i}BVE hard segments, rendered by the sterically demanding chiral counterion derived from IDPi-**1**, are crucial to achieve enhanced mechanical property of the PDHF$_{2000}$-P^{i}BVE$_{6000}$ gradient copolymer, which might have originated from the favored microphase separation (Figure S18).

Thanks to all-carbon backbones, the PDHF$_{2000}$-P^{i}BVE$_{6000}$ TPE has been demonstrated to have high thermal stability, as indicated by a high onset degradation temperature (T_d, defined by the temperatures of 5% weight loss) of 309 °C in thermal gravimetric analysis (TGA, Figure 6B). This T_d value is identical to that of isotactic P^{i}BVE (316 °C) but 40 °C lower than that of PDHF (349 °C). Remarkably, in sharp contrast to the conventional carbon-backbone polymers that are generally resistant to degradation, DHF/^{i}BVE gradient copolymers obtained in this study are capable of degradation under certain external stimuli. In the presence of Fenton reagent comprising hydrogen peroxide and divalent iron salt [$(NH_4)_2Fe(SO_4)_2 \cdot 6H_2O$], which has shown to have the ability to trigger an accelerated oxidative degradation of PDHF, as established by Fors and co-workers,[26] fast degradation of PDHF$_{2000}$-P^{i}BVE$_{6000}$ was achieved in first 1 h, where a significant decrease of M_n from 296.4 to 32.8 kg/mol was observed without any detectable residual polymers (Table S4 and Figure 6C,D). After that, the degradation became slow in which M_n gradually reduced to 5.3 kg/mol within 24 h, and further extending the degradation time to 168 h led to a decrease of M_n to 1.8 kg/mol. The analysis of the resultant degradation product by NMR (Figures S19 and S20) confirmed that the degradation follows the same oxidative mechanism as PDHF degradation,[26] as the observation of the characteristic signals of carboxylic acid at 9.75 ppm and aldehyde at 8.75 ppm in the ^{1}H NMR spectrum as well as > C═O at 176.7 ppm in the ^{13}C NMR spectrum. Switching to the PDHF$_{1600}$-P^{i}BVE$_{6400}$ gradient copolymer, similar degradation kinetics was observed, and its M_n can finally reduce to 1.6 kg/mol in 168 h (Table S4 and Figure S21). It was found that, under the same conditions, the degradation rate of DHF/^{i}BVE gradient copolymers is slower than that of the PDHF homopolymer in which the decrease of M_n to 1.9 kg/mol was accomplished within 48 h (Figure 6C and Table S4).[26] Moreover, DHF/^{i}BVE gradient copolymers and the PDHF homopolymer all exhibited much faster degradation rates than that of the isotactic P^{i}BVE homopolymer (Table S4 and Figure 6C), indicating that the existence of the DHF unit in the polymer can significantly accelerate the degradation. It is speculated that the hydrogen atom transfer (HAT) process, triggered by oxidizing hydroxyl radical species generated by Fenton reagent, is much more readily for the cyclic DHF unit than for the linear ^{i}BVE unit.

■ CONCLUSIONS

In summary, the facile synthesis of carbon-backbone TPEs has been established in this work via a one-step cationic copolymerization from biorenewable ^{i}BVE and DHF monomer mixtures. By utilization of a strong organic Brønsted acid IDPi-**1** as the single-component organic catalyst, the polymerization rate of DHF is much faster than that of ^{i}BVE during the copolymerization as opposed to their homopolymerization rates (^{i}BVE ≫ DHF), presumably due to facilitating initiation by ^{i}BVE. Accordingly, DHF/^{i}BVE gradient copolymers consisting of DHF-rich, ^{i}BVE-rich, and neat-P^{i}BVE segments have been conveniently synthesized in a one-step approach. Moreover, the sterically demanding chiral counterion derived from IDPi-**1** not only allows the copolymerization to proceed in a relatively controlled way presumably due to the stabilization of carbocation propagation species via ion-pair interaction but also renders isotactic P^{i}BVE segments to afford a hard−soft−hard structure for high-performance TPEs. Finally, PDHF$_{2000}$-P^{i}BVE$_{6000}$ has been demonstrated to possess good thermal (T_d = 309 °C, T_m ≈ 70 °C, T_g ≈ −16 to 30 °C) and elastomeric properties (σ_B = 5.73 MPa, ε_B = 880%) yet capable of degrading in the presence of Fenton reagent, thus successfully affording a new carbon-backbone TPE with high performance and on-demand degradability for the first time from poly(vinyl ether)-based gradient copolymers. Optimization of the IDPi catalyst for achieving more precise control on monomer sequence as well as the conversion of oligomeric degradation products into recyclable building blocks are currently underway.

■ ASSOCIATED CONTENT

Supporting Information

The Supporting Information is available free of charge at https://pubs.acs.org/doi/10.1021/acs.macromol.4c00857.

Experimental details, materials, and characterizations; kinetic studies of homopolymerization and copolymerization; measurement of reactivity ratios of DHF and ^{i}BVE; GPC curves of gradient copolymer samples with high MWs; quantitative ^{13}C NMR spectra of homopolymers and gradient copolymers; first-heating-scan DSC curves, WXRD profiles, AFM image, and stress−strain curves of gradient copolymers; and NMR spectra of the degradation product of gradient copolymers (PDF)

■ AUTHOR INFORMATION

Corresponding Authors

Yanping Zhang − *State Key Laboratory of Organometallic Chemistry, Shanghai Institute of Organic Chemistry, University of Chinese Academy of Sciences, Chinese Academy of Sciences, Shanghai 200032, China*; Email: yanpingzh@sioc.ac.cn

Miao Hong − *State Key Laboratory of Organometallic Chemistry, Shanghai Institute of Organic Chemistry, University of Chinese Academy of Sciences, Chinese Academy of Sciences, Shanghai 200032, China; School of Chemistry and Material Sciences, Hangzhou Institute for Advanced Study, University of Chinese Academy of Sciences, Hangzhou 310024, China;* orcid.org/0000-0003-1016-882X; Email: miaohong@sioc.ac.cn

Authors

Yuqin Zhou − *State Key Laboratory of Organometallic Chemistry, Shanghai Institute of Organic Chemistry, University of Chinese Academy of Sciences, Chinese Academy of Sciences, Shanghai 200032, China*

Yangyang Sun − *State Key Laboratory of Organometallic Chemistry, Shanghai Institute of Organic Chemistry, University of Chinese Academy of Sciences, Chinese Academy of Sciences, Shanghai 200032, China*

Complete contact information is available at: https://pubs.acs.org/10.1021/acs.macromol.4c00857

https://doi.org/10.1021/acs.macromol.4c00857
Macromolecules 2024, 57, 7227−7236

Notes

The authors declare no competing financial interest.

■ ACKNOWLEDGMENTS

This work was supported by the National Key R&D Program of China (2021YFA1501700), National Natural Science Foundation of China (Grant Nos. 21821002, 52203020, and 22201292), the Science and Technology Commission of Shanghai Municipality (Grant Nos. 22ZR1481900, 23XD1424600, and 22YF1458100), the Strategic Priority Research Program of the Chinese Academy of Sciences (Grant No. XDB0610000), and the CAS Project for Young Scientists in Basic Research (Grant No. YSBR-094). Dr. Y.S. is thankful for the financial support from the Youth Innovation Promotion Association CAS (2022253).

■ REFERENCES

(1) Bates, F. S.; Hillmyer, M. A.; Lodge, T. P.; Bates, C. M.; Delaney, K. T.; Fredrickson, G. H. Multiblock Polymers: Panacea or Pandora's Box? *Science* **2012**, *336*, 434−440.

(2) Mohite, A. S.; Rajpurkar, Y. D.; More, A. P. Bridging the Gap Between Rubbers and Plastics: a Review on Thermoplastic Polyolefin Elastomers. *Polym. Bull.* **2022**, *79*, 1309−1343.

(3) Handlin, D. L., Jr; Trenor, S.; Wright, K. Applications of Thermoplastic Elastomers Based on Styrenic Block Copolymers. *Macromol. Eng.* **2007**, 2001−2031, DOI: 10.1002/9783527631421.ch48.

(4) Spontak, R. J.; Patel, N. P. Thermoplastic Elastomers: Fundamentals and Applications. *Curr. Opin. Colloid Interface Sci.* **2000**, *5*, 333−340.

(5) The Future of Thermoplastic Elastomers to 2026. https://www.smithers.com/services/market-reports/materials/the-future-of-thermoplastic-elastomers-to-2026 (accessed Dec 21, 2023).

(6) Whelan, D. Thermoplastic Elastomers. In *Brydson's Plastics Materials*, 8th ed.; Gilbert, M., Ed.; Butterworth-Heinemann, 2017; pp 653−703.

(7) Xiong, M.; Schneiderman, D. K.; Bates, F. S.; Hillmyer, M. A.; Zhang, K. Scalable Production of Mechanically Tunable Block Polymers from Sugar. *Proc. Natl. Acad. Sci. U.S.A.* **2014**, *111*, 8357−8362.

(8) Hillmyer, M. A.; Tolman, W. B. Aliphatic Polyester Block Polymers: Renewable, Degradable, and Sustainable. *Acc. Chem. Res.* **2014**, *47*, 2390−2396.

(9) Zhu, Y.; Radlauer, M. R.; Schneiderman, D. K.; Shaffer, M. S. P.; Hillmyer, M. A.; Williams, C. K. Multiblock Polyesters Demonstrating High Elasticity and Shape Memory Effects. *Macromolecules* **2018**, *51*, 2466−2475.

(10) Li, C.; Wang, L.; Yan, Q.; Liu, F.; Shen, Y.; Li, Z. Rapid and Controlled Polymerization of Bio-sourced δ-Caprolactone toward Fully Recyclable Polyesters and Thermoplastic Elastomers. *Angew. Chem., Int. Ed.* **2022**, *61*, No. e202201407.

(11) Yan, Q.; Li, C.; Yan, T.; Shen, Y.; Li, Z. Chemically Recyclable Thermoplastic Polyurethane Elastomers via a Cascade Ring-Opening and Step-Growth Polymerization Strategy from Bio-renewable δ-Caprolactone. *Macromolecules* **2022**, *55*, 3860−3868.

(12) Zhao, W.; Li, C.; Yang, X.; He, J.; Pang, X.; Zhang, Y.; Men, Y.; Chen, X. One-Pot Synthesis of Supertough, Sustainable Polyester Thermoplastic Elastomers Using Block-Like, Gradient Copolymer as Soft Midblock. *CCS Chem.* **2022**, *4*, 1263−1272.

(13) Hada, R.; Kanazawa, A.; Aoshima, S. Degradable Silyl Ether Polymers Synthesized by Sequence-Controlled Cationic Terpolymerization of 1,3-Dioxa-2-silacycloalkanes with Vinyl Ethers and Aldehydes. *Macromolecules* **2022**, *55*, 5474−5484.

(14) Coates, G. W.; Waymouth, R. M. Oscillating Stereocontrol: A Strategy for the Synthesis of Thermoplastic Elastomeric Polypropylene. *Science* **1995**, *267* (5195), 217−219.

(15) Arriola, D. J.; Carnahan, E. M.; Hustad, P. D.; Kuhlman, R. L.; Wenzel, T. T. Catalytic Production of Olefin Block Copolymers via Chain Shuttling Polymerization. *Science* **2006**, *312*, 714−719.

(16) Reilly, L. T.; McGraw, M. L.; Eckstrom, F. D.; Clarke, R. W.; Franklin, K. A.; Chokkapu, E. R.; Cavallo, L.; Falivene, L.; Chen, E. Y. X. Compounded Interplay of Kinetic and Thermodynamic Control over Comonomer Sequences by Lewis Pair Polymerization. *J. Am. Chem. Soc.* **2022**, *144* (51), 23572−23584.

(17) McGraw, M. L.; Clarke, R. W.; Chen, E. Y.-X. Compounded Sequence Control in Polymerization of One-Pot Mixtures of Highly Reactive Acrylates by Differentiating Lewis Pairs. *J. Am. Chem. Soc.* **2020**, *142*, 5969−5973.

(18) Wan, Y.; He, J.; Zhang, Y.; Chen, E. Y.-X. One-Step Synthesis of Lignin-Based Triblock Copolymers as High-Temperature and UV-Blocking Thermoplastic Elastomers. *Angew. Chem., Int. Ed.* **2022**, *61*, No. e202114946.

(19) Gregory, G. L.; Sulley, G. S.; Carrodeguas, L. P.; Chen, T. T. D.; Santmarti, A.; Terrill, N. J.; Lee, K.-Y.; Williams, C. K. Triblock Polyester Thermoplastic Elastomers with Semi-Aromatic Polymer End Blocks by Ring-Opening Copolymerization. *Chem. Sci.* **2020**, *11*, 6567−6581.

(20) Sulley, G. S.; Gregory, G. L.; Chen, T. T. D.; Carrodeguas, L. P.; Trott, G.; Santmarti, A.; Lee, K.-Y.; Terrill, N. J.; Williams, C. K. Switchable Catalysis Improves the Properties of CO_2-Derived Polymers: Poly(cyclohexene carbonate-*b*-ε-decalactone-*b*-cyclohexene carbonate) Adhesives, Elastomers, and Toughened Plastics. *J. Am. Chem. Soc.* **2020**, *142*, 4367−4378.

(21) Poon, K. C.; Gregory, G. L.; Sulley, G. S.; Vidal, F.; Williams, C. K. Toughening CO_2-Derived Copolymer Elastomers Through Ionomer Networking. *Adv. Mater.* **2023**, *35*, No. e2312069.

(22) Ji, H.; Wang, B.; Pan, L.; Li, Y. One-Step Access to Sequence-Controlled Block Copolymers by Self-Switchable Organocatalytic Multicomponent Polymerization. *Angew. Chem., Int. Ed.* **2018**, *57*, 16888−16892.

(23) Hu, C.; Pang, X.; Chen, X. Self-Switchable Polymerization: A Smart Approach to Sequence-Controlled Degradable Copolymers. *Macromolecules* **2022**, *55*, 1879−1893.

(24) Matake, R.; Adachi, Y.; Matsubara, H. Synthesis of Vinyl Ethers of Alcohols Using Calcium Carbide Under Superbasic Catalytic Conditions (KOH/DMSO). *Green Chem.* **2016**, *18*, 2614−2618.

(25) Spring, S. W.; Smith-Sweetser, R. O.; Rosenbloom, S. I.; Sifri, R. J.; Fors, B. P. Sustainable Thermoplastic Elastomers Produced via Cationic RAFT Polymerization. *Polym. Chem.* **2021**, *12*, 1097−1104.

(26) Spring, S. W.; Hsu, J. H.; Sifri, R. J.; Yang, S. M.; Cerione, C. S.; Lambert, T. H.; Ellison, C. J.; Fors, B. P. Poly(2,3-Dihydrofuran): A Strong, Biorenewable, and Degradable Thermoplastic Synthesized via Room Temperature Cationic Polymerization. *J. Am. Chem. Soc.* **2022**, *144*, 15727−15734.

(27) Kimura, T.; Ouchi, M. Photocatalyzed Hydrogen Atom Transfer Degradation of Vinyl Polymers: Cleavage of a Backbone C−C Bond Triggered by Radical Activation of a C−H Bond in a Pendant. *Angew. Chem., Int. Ed.* **2023**, *62*, No. e202305252.

(28) Schreyer, L.; Properzi, R.; List, B. IDPi Catalysis. *Angew. Chem., Int. Ed.* **2019**, *58*, 12761−12777.

(29) Mitschke, B.; Turberg, M.; List, B. Confinement as a Unifying Element in Selective Catalysis. *Chem.* **2020**, *6*, 2515−2532.

(30) Amatov, T.; Tsuji, N.; Maji, R.; Schreyer, L.; Zhou, H.; Leutzsch, M.; List, B. Confinement-Controlled, Either syn- or anti-Selective Catalytic Asymmetric Mukaiyama Aldolizations of Propionaldehyde Enolsilanes. *J. Am. Chem. Soc.* **2021**, *143*, 14475−14481.

(31) Ouyang, J.; Maji, R.; Leutzsch, M.; Mitschke, B.; List, B. Design of an Organocatalytic Asymmetric (4 + 3) Cycloaddition of 2-Indolylalcohols with Dienolsilanes. *J. Am. Chem. Soc.* **2022**, *144*, 8460−8466.

(32) Wakchaure, V. N.; DeSnoo, W.; Laconsay, C. J.; Leutzsch, M.; Tsuji, N.; Tantillo, D. J.; List, B. Catalytic Asymmetric Cationic Shifts of Aliphatic Hydrocarbons. *Nature* **2024**, *625*, 287−292.

(33) Knutson, P. C.; Teator, A. J.; Varner, T. P.; Kozuszek, C. T.; Jacky, P. E.; Leibfarth, F. A. Bronsted Acid Catalyzed Stereoselective

Polymerization of Vinyl Ethers. *J. Am. Chem. Soc.* **2021**, *143*, 16388−16393.
(34) Yang, Z.; Zhang, X.; Jiang, Y.; Ma, Q.; Liao, S. Organocatalytic Stereoselective Cationic Polymerization of Vinyl Ethers by Employing a Confined Brønsted Acid as the Catalyst. *Sci. China Chem.* **2022**, *65*, 304−308.
(35) Gatzenmeier, T.; Kaib, P. S. J.; Lingnau, J. B.; Goddard, R.; List, B. The Catalytic Asymmetric Mukaiyama-Michael Reaction of Silyl Ketene Acetals with α,β-Unsaturated Methyl Esters. *Angew. Chem., Int. Ed.* **2018**, *57*, 2464−2468.
(36) Lee, S.; Kaib, P. S. J.; List, B. Asymmetric Catalysis via Cyclic, Aliphatic Oxocarbenium Ions. *J. Am. Chem. Soc.* **2017**, *139*, 2156−2159.
(37) Watanabe, H.; Kanazawa, A.; Okumoto, S.; Aoshima, S. Role of the Counteranion in the Stereospecific Living Cationic Polymerization of *N*-Vinylcarbazole and Vinyl Ethers: Mechanistic Investigation and Synthesis of Stereo-Designed Polymers. *Macromolecules* **2022**, *55*, 4378−4388.
(38) Beckingham, B. S.; Sanoja, G. E.; Lynd, N. A. Simple and Accurate Determination of Reactivity Ratios Using a Nonterminal Model of Chain Copolymerization. *Macromolecules* **2015**, *48*, 6922−6930.
(39) Lynd, N. A.; Ferrier, R. C.; Beckingham, B. S. Recommendation for Accurate Experimental Determination of Reactivity Ratios in Chain Copolymerization. *Macromolecules* **2019**, *52*, 2277−2285.
(40) Blankenburg, J.; Kersten, E.; Maciol, K.; Wagner, M.; Zarbakhsh, S.; Frey, H. The Poly(propylene oxide-co-ethylene oxide) Gradient Is Controlled by the Polymerization Method: Determination of Reactivity Ratios by Direct Comparison of Different Copolymerization Models. *Polym. Chem.* **2019**, *10*, 2863−2871.
(41) Gleede, T.; Markwart, J. C.; Huber, N.; Rieger, E.; Wurm, F. R. Competitive Copolymerization: Access to Aziridine Copolymers with Adjustable Gradient Strengths. *Macromolecules* **2019**, *52*, 9703−9714.
(42) Kersten, E.; Linker, O.; Blankenburg, J.; Wagner, M.; Walther, P.; Naumann, S.; Frey, H. Revealing the Monomer Gradient of Polyether Copolymers Prepared Using *N*-Heterocyclic Olefins: Metal-Free Anionic versus Zwitterionic Lewis Pair Polymerization. *Macromol. Chem. Phys.* **2023**, *224*, No. 2300097.
(43) Teator, A. J.; Leibfarth, F. A. Catalyst-Controlled Stereoselective Cationic Polymerization of Vinyl Ethers. *Science* **2019**, *363*, 1439−1443.
(44) Teator, A. J.; Varner, T. P.; Jacky, P. E.; Sheyko, K. A.; Leibfarth, F. A. Polar Thermoplastics with Tunable Physical Properties Enabled by the Stereoselective Copolymerization of Vinyl Ethers. *ACS Macro Lett.* **2019**, *8*, 1559−1563.
(45) Mizuno, N.; Satoh, K.; Kamigaito, M.; Okamoto, Y. Living Cationic Polymerization of a Novel Bicyclic Conjugated Diene Monomer, Tetrahydroindene, and Its Block Copolymers with Vinyl Ether. *Macromolecules* **2006**, *39*, 5280−5285.
(46) Imaeda, T.; Hashimoto, T.; Irie, S.; Urushisaki, M.; Sakaguchi, T. Synthesis of ABA-triblock and Star-diblock Copolymers with Poly(2-adamantyl vinyl ether) and Poly(N-butyl vinyl ether) Segments: New Thermoplastic Elastomers Composed Solely of Poly(vinyl ether) backbones. *J. Polym. Sci., Part A: Polym. Chem.* **2013**, *51*, 1796−1807.
(47) Brostow, W. Mechanical Properties. In *Physical Properties of Polymers Handbook*; Mark, J. E., Ed.; Springer New York: New York, NY, 2007; pp 423−445.
(48) Alam, M. M.; Jack, K. S.; Hill, D. J. T.; Whittaker, A. K.; Peng, H. Gradient Copolymers − Preparation, Properties and Practice. *Eur. Polym. J.* **2019**, *116*, 394−414.
(49) Guo, Y.; Gao, X.; Luo, Y. Mechanical Properties of Gradient Copolymers of Styrene and n-Butyl Acrylate. *J. Polym. Sci., Part B: Polym. Phys.* **2015**, *53*, 860−868.
(50) Jouenne, S.; González-León, J. A.; Ruzette, A.-V.; Lodefier, P.; Tencé-Girault, S.; Leibler, L. Styrene/Butadiene Gradient Block Copolymers: Molecular and Mesoscopic Structures. *Macromolecules* **2007**, *40*, 2432−2442.
(51) Hodrokoukes, P.; Floudas, G.; Pispas, S.; Hadjichristidis, N. Microphase Separation in Normal and Inverse Tapered Block Copolymers of Polystyrene and Polyisoprene. 1. Phase State. *Macromolecules* **2001**, *34*, 650−657.

https://doi.org/10.1021/acs.macromol.4c00857
Macromolecules 2024, 57, 7227−7236